Water Science and Engineering 2016, 9(2): 87–96

HOSTED BY

ELSEVIER

CrossMark

Available online at www.sciencedirect.com

Water Science and Engineering

journal homepage: http://www.waterjournal.cn

Evaluation of latest TMPA and CMORPH satellite precipitation products over Yellow River Basin

Shan-hu Jiang [a,b], Meng Zhou [a,b], Li-liang Ren [a,*], Xue-rong Cheng [a,b], Peng-ju Zhang [b]

[a] *State Key Laboratory of Hydrology-Water Resources and Hydraulic Engineering, Hohai University, Nanjing 210098, China*
[b] *College of Hydrology and Water Resources, Hohai University, Nanjing 210098, China*

Received 28 September 2015; accepted 17 March 2016
Available online 15 June 2016

Abstract

The main objective of this study was to evaluate four latest global high-resolution satellite precipitation products (TMPA 3B42RT, CMORPH, TMPA 3B42V7, and CMORPH_adj) against gauge observations of the Yellow River Basin from March 2000 to December 2012. The assessment was conducted with several commonly used statistical indices at daily and monthly scales. Results indicate that 3B42V7 and CMORPH_adj perform better than the near real-time products (3B42RT and CMORPH), particularly the 3B42V7 product. The adjustment by gauge data significantly reduces the systematic biases in the research products. Regarding the near real-time datasets, 3B42RT overestimates rainfall over the whole basin, while CMORPH presents a mixed pattern with negative and positive values of relative bias in low- and high-latitude regions, respectively, and CMORPH performs better than 3B42RT on the whole. According to the spatial distribution of statistical indices, these values are optimized in the southeast and decrease toward the northwest, and the trend is similar for the spatial distribution of the mean annual precipitation during the period from 2000 to 2012. This study also reveals that all the four products can effectively detect rainfall events. This study provides useful information about four mainstream satellite products in the Yellow River Basin, and the findings can facilitate the use of global precipitation measurement (GPM) data in the future.

Keywords: Satellite precipitation; TMPA; CMORPH; Yellow River Basin

1. Introduction

Precipitation is the most important atmospheric input for a terrestrial hydrologic system, and the variability of this input is a critical component of both hydrological processes and energy cycles (Tong et al., 2014). Precipitation must be measured accurately for water resources applications and hydrologic monitoring. Traditionally, ground-based rain gauge networks and radar are the major tools used for rainfall observations. However, rain gauges are distributed sparsely and unevenly, and they are always insufficient for areas with complex terrain. In addition, despite the high resolution of the radar dataset, the data quality is reduced in such terrain as a result of the distorted electronic signals introduced by the surrounding environment (Li et al., 2013). To overcome the limitations of rain gauges and radar precipitation estimation, satellite-based precipitation estimation has been developed as another approach. Thus far, a number of high-resolution satellite precipitation products have been developed, including TRMM multi-satellite precipitation analysis (TMPA) (Huffman et al., 2007), the Climate Prediction Center morphing technique (CMORPH) (Joyce et al., 2004), and others. The Core Observatory of Global Precipitation Measurement (GPM) was launched on February 27, 2014. The

This work was supported by the Programme of Introducing Talents of Discipline to Universities (the 111 Project, Grant No. B08048), the National Natural Science Foundation of China (Grant No. 41501017), and the Natural Science Foundation of Jiangsu Province (Grant No. BK20150815).
* Corresponding author.
E-mail address: njRLL9999@126.com (Li-liang Ren).
Peer review under responsibility of Hohai University.

http://dx.doi.org/10.1016/j.wse.2016.06.002

GPM mission aims to establish accurate global precipitation products with high spatial and temporal resolutions for users (Yong et al., 2015). Satellite precipitation retrieval has progressed from the TRMM era to the GPM era. Prior to the release of GPM data, the algorithms for TMPA and CMORPH were updated and their latest data were released. Thus, evaluating the most recent TMPA and CMORPH satellite precipitation data provides a reference for the application of GPM data.

In recent years, various satellite products have been validated globally and regionally, and the TMPA and CMORPH have been found to be the two better performing satellite precipitation products in the TRMM era (Cai et al., 2014; Ferreira et al., 2014; Lo Conti et al., 2014; Hu et al., 2014; Jiang et al., 2010; Li et al., 2012; Liu, 2015; Nastos et al., 2013; Petersen and Rutledge, 2001; Sadiq et al., 2014; Shen et al., 2010, 2014; Xue et al., 2013; Yong et al., 2010, 2014). Jiang et al. (2010) evaluated three high-resolution satellite precipitation products (TRMM 3B42V6, TRMM 3B42RT, and CMORPH) against surface rain gauge observations across the Laohahe Basin in northern China and pointed out that 3B42V6 corresponds best with the surface observations. Moreover, CMORPH performs significantly better than 3B42RT. Li et al. (2015) evaluated four mainstream global satellite precipitation products (TRMM 3B42V7, TRMM 3B42RT, CMORPH, and PERSIANN) for multi-scale hydrologic application in the Yangtze River Basin and concluded that the gauge adjustment greatly reduces the bias in the research-grade TMPA product 3B42V7, but this product is not always superior to other products (particularly CMORPH) at the daily scale. The performance of 3B42V7 is comparable to the data from the China Meteorological Administration (CMA) at both the monthly and daily scales, mainly due to the monthly gauge adjustment. Nonetheless, CMORPH performs better than TMPA in some regions. Therefore, we compared four mainstream global high-resolution satellite precipitation products (TMPA 3B42RT, CMORPH, TMPA 3B42V7, and CMORPH_adj) against gauge observations obtained from the CMA.

The Yellow River Basin, which is the second-largest river basin in China, has complex topography and sparse rain gauge observation networks (Meng et al., 2014; Hao et al., 2014). The satellite precipitation data have important implications for local climate monitoring and hydrological application. Meng et al. (2014) quantitatively assessed TMPA 3B42V6 against the gauged rainfall during the period from 1998 to 2008 in the source region of the Yellow River Basin, and concluded that the validation indices of TMPA were closely associated with latitude and annual precipitation. Hao et al. (2014) evaluated the streamflow simulation utility of the TMPA data and suggested that the 3B42V7 is capable of performing daily streamflow simulation in the upper Yellow River Basin. These two studies have provided some references for the use of TMPA data in the upper Yellow River Basin, while the performance of the latest TMPA and CMORPH products throughout the Yellow River Basin is still unknown. Therefore, the objective of the present study was to comprehensively evaluate the four latest high-resolution satellite precipitation products, namely, TMPA 3B42V7, TMPA 3B42RT, CMORPH, and CMORPH_adj, throughout the Yellow River Basin.

2. Study region

The Yellow River has a drainage area of 7.95×10^5 km^2 and originates on the eastern Tibet Plateau. The middle reaches flow across the Loess Plateau, and the lower reaches flow across a fluvial plain before debouching into the Bohai Sea. The basin is located in the northern area of China; it extends from 96°E to 119°E in longitude and from 32°N to 42°N in latitude. The Yellow River Basin is one of the most important basins in China and directly supports a population of 107 million people. The elevation within the basin ranges from 1 m to 6199 m and declines from west to east. In addition, the river flows across arid, semi-arid, and semi-humid regions. The average temperature ranges from approximately −4°C to 14°C, and the mean annual precipitation is roughly 466 mm. The temporal and spatial distributions of the precipitation within the basin are inhomogeneous. The precipitation increases from northwest to southeast. Moreover, the majority of the annual precipitation falls between June and September.

The precipitation input must be accurate to show the changes in the regional hydrological cycle as well as to monitor regional flood and drought disasters. This study aimed to evaluate four satellite precipitation products over this basin. To assess the regional performance, we divided the entire basin into 14 sub-basins according to the drainage system (Fig. 1).

3. Data and methodology

3.1. Satellite precipitation data

Four high-resolution satellite precipitation data sets (TMPA 3B42RT, CMORPH, TMPA 3B42V7, and CMORPH_adj) during the period from March 2000 to December 2012 were used in this study.

The most recently released version of TMPA products (version 7), 3B42RT and 3B42V7, were used in this study. The former is less accurate than the latter although it generates quick precipitation estimates for near real-time modeling and monitoring activities. The algorithm for the latter was calibrated with gauge data, different sensor calibrations, and additional post-processing, thus resulting in a two-month delay (Liu, 2015; Huffman et al., 2007). Nonetheless, the research product is accurate and suitable for the present work. Both products share a 0.25° × 0.25° grid. However, their initiation dates are different. 3B42RT has been available since March 1, 2000, whereas 3B42V7 was released on January 1, 1998. Therefore, these products were compared in the period beginning from March 2000 in this study.

CMORPH products are derived via the morphing technique that uses the precipitation estimates derived from passive microwave observations (Joyce et al., 2004). The CMORPH

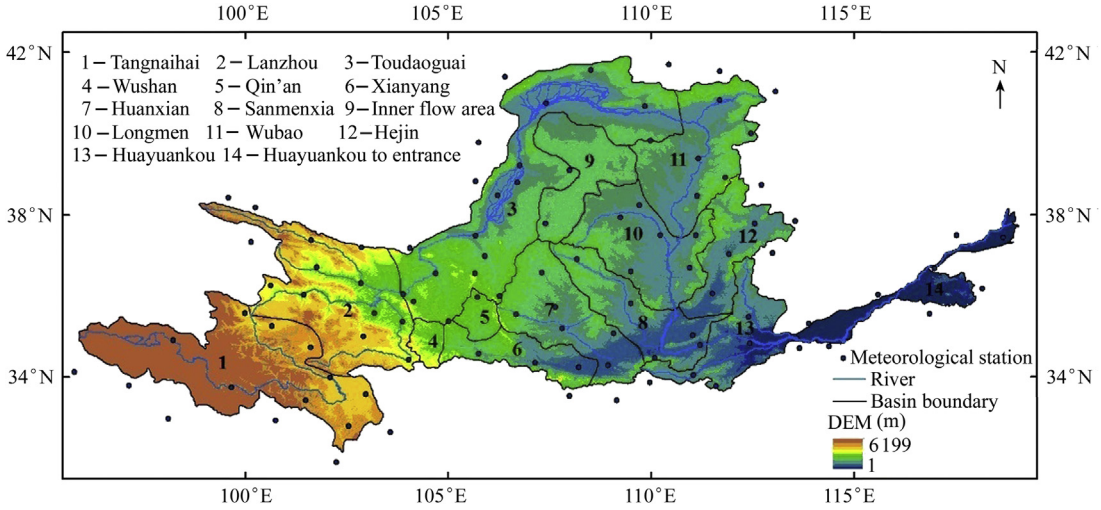

Fig. 1. Locations of Yellow River Basin and sub-basins.

products used in this study are generated on 0.25° spatial grids every 3 h with coverage from 60°S to 60°N. CMORPH has been available since January 1, 1998. Moreover, CMORPH adjustment is the result of calibration with rain gauge data. The temporal and spatial resolutions are similar in this case.

To evaluate the daily and monthly satellite precipitation products, satellite precipitation products with a temporal resolution of 3 h were aggregated to produce the accumulated daily and monthly precipitation.

3.2. Gauged precipitation data

The CMA provided the daily observational precipitation data from 101 meteorological stations located in the Yellow River Basin. To facilitate direct comparison with the satellite data, we interpolated the data from the 101 stations into a spatial distribution with a 0.25° × 0.25° resolution using the inverse distance weighting interpolation method (Bartier and Keller, 1996), which has been proven to be an efficient and consistent approach by many studies (Chen and Liu, 2012; Zhuang and Wang, 2003).

3.3. Evaluation statistics

To quantitatively evaluate the satellite precipitation products against the rain gauge data, four widely used statistical validation indices were adopted in this study. Relative bias (BIAS) describes the systematic bias of the satellite precipitation. Mean error (ME) measures the average magnitude of the error. Although a root mean square error (RMSE) also determines the average error magnitude, this indicator assigns greater weight to large errors than ME does. The correlation coefficient (CC) was used to assess the agreement between the satellite precipitation and rain gauge observations (Jiang et al., 2010).

As for the contingency table statistics, we computed the probability of detection (POD), false alarm rate (FAR), and critical success index (CSI) values to determine the correspondence between the estimated and observed occurrences of rainfall events (Ebert et al., 2007).

4. Results and discussion

4.1. Comparison at 0.25° × 0.25° grid scale

To compare the satellite precipitation products with the ground rain gauge observations at the 0.25° × 0.25° spatial scale, we computed seven accuracy indices at daily and monthly time scales, as shown in Table 1. At the daily scale, the BIAS ranges from 5.10% to 48.65%, which indicates that all the satellite precipitation products overestimated precipitation, particularly the 3B42RT. Correspondingly, 3B42RT reports the largest ME and RMSE values. All the satellite precipitation products exhibit a low correlation with ground rain gauge data, and the CC value ranges from 0.27 (for 3B42RT) to 0.35 (for 3B42V7). The POD indices for 3B42RT, CMORPH, and CMORPH_adj are similar and are better than 3B42V7 at detecting rainfall events. In addition, the CSI values for all the data sets are similar, and the FAR value for 3B42V7 has a slight decrease. Therefore, the values of the three categorical statistics (POD, CSI, and FAR) suggest that all four satellite precipitation products detect rainfall events well in the Yellow River Basin.

As with the daily results, the collected monthly satellite data also overestimated precipitation; the trend decreases from 3B42RT, CMORPH_adj, and 3B42V7 to CMORPH. The CC value of 3B42V7 (0.91) against the rain gauge data is higher than those of 3B42RT (0.71), CMORPH (0.72), and CMORPH_adj (0.83). Thus, 3B42V7 generates the best monthly precipitation estimates.

Figs. 2 through 5 show the spatial distributions of BIAS, ME, CC, and POD; these values were computed from the daily precipitation datasets of four satellite products and compared with rain gauge observations on a 0.25° × 0.25° grid. The BIAS and

Table 1
Statistical summary of grid-based comparison of four satellite precipitation estimates in Yellow River Basin at daily and monthly scales.

Satellite precipitation product	Statistical index at daily scale							Statistical index at monthly scale			
	BIAS (%)	ME (mm)	RMSE (mm)	CC	POD	FAR	CSI	BIAS (%)	ME (mm)	RMSE (mm)	CC
TMPA 3B42RT	48.65	0.55	6.12	0.27	0.46	0.60	0.27	48.65	16.75	42.09	0.71
CMORPH	5.10	0.00	4.42	0.30	0.46	0.61	0.27	5.10	0.14	28.15	0.72
TMPA 3B42V7	8.93	0.10	4.72	0.35	0.44	0.56	0.28	8.93	3.03	17.07	0.91
CMORPH_adj	12.23	0.12	4.69	0.32	0.47	0.57	0.29	12.23	3.74	24.40	0.83

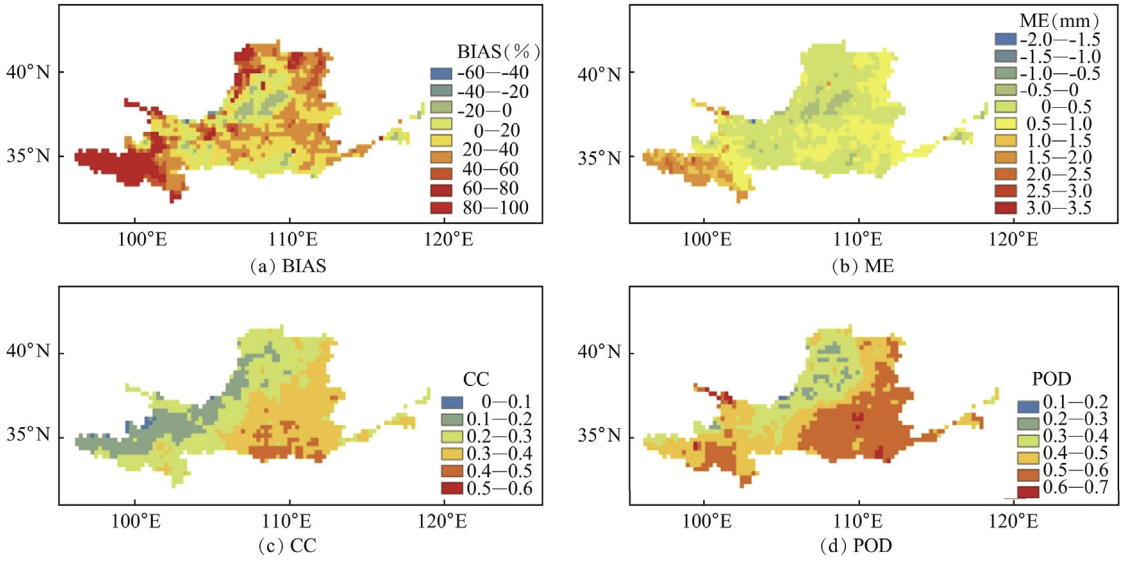

Fig. 2. Spatial distributions of statistical indices computed from daily precipitation data obtained with 3B42RT throughout Yellow River Basin.

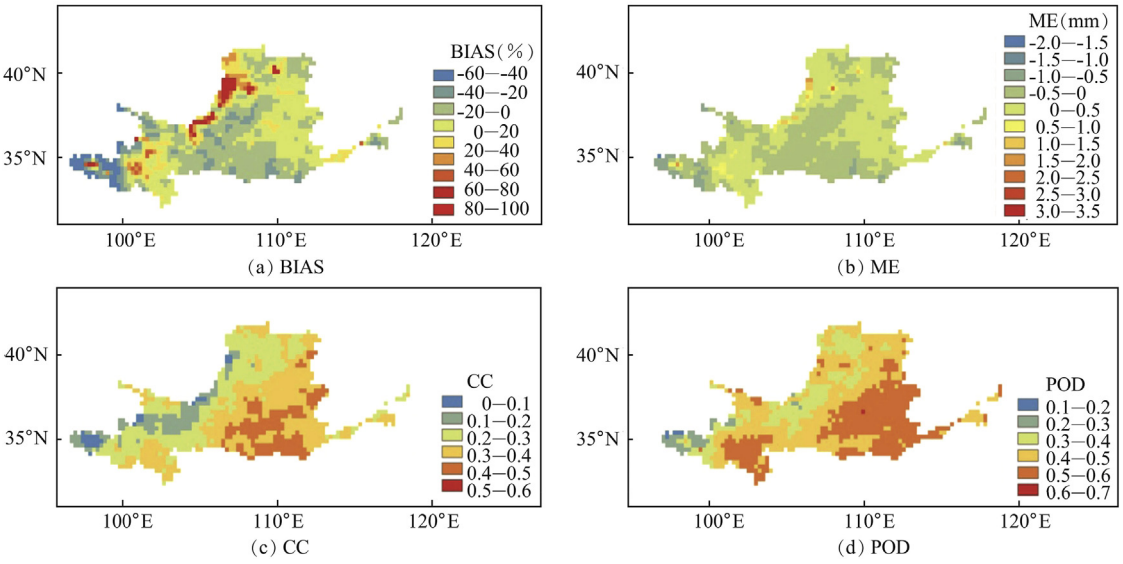

Fig. 3. Spatial distributions of statistical indices computed from daily precipitation data obtained with CMORPH throughout Yellow River Basin.

ME values of 3B42RT are significantly higher than those of the other products across the entire basin. CMORPH presents a mixed pattern, with negative and positive BIAS values in the low- and high-latitude regions, respectively. Meanwhile, the other three products overestimate the precipitation in most parts of the basin. All the spatial distributions of CC and POD exhibit a similar pattern. These figures also show that the values are optimized in the southeast and decrease toward the northwest, and the trend is

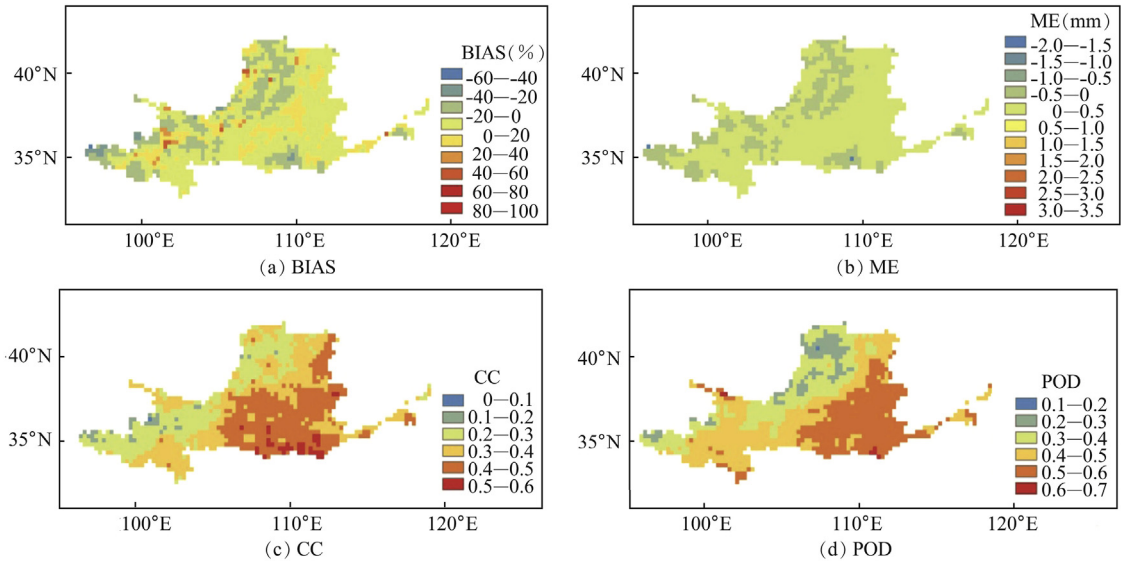

Fig. 4. Spatial distributions of statistical indices computed from daily precipitation data obtained with 3B42V7 throughout Yellow River Basin.

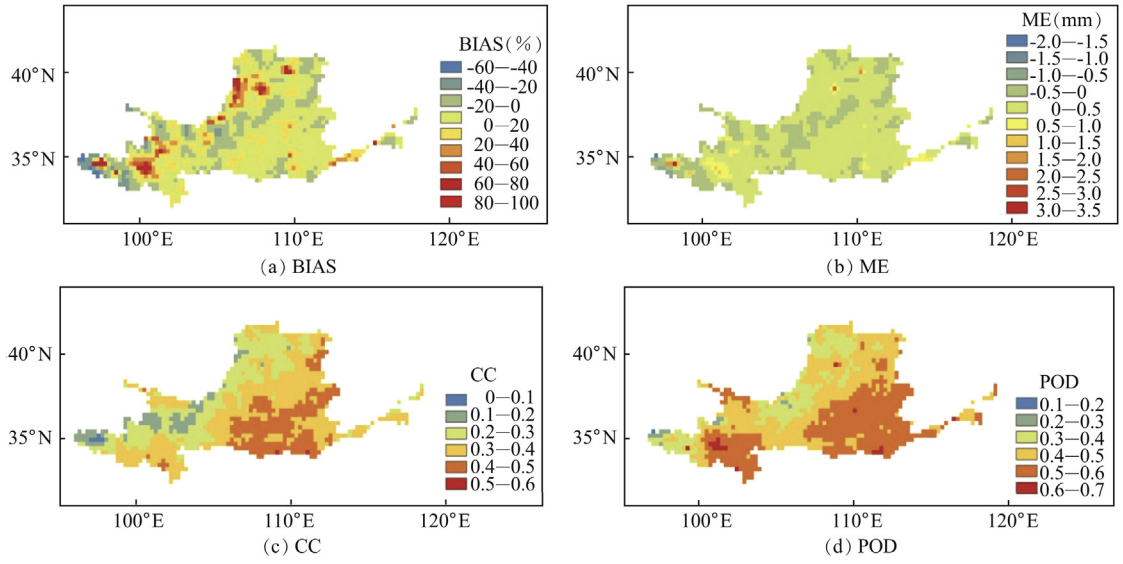

Fig. 5. Spatial distributions of statistical indices computed from daily precipitation data obtained with CMORPH_adj throughout Yellow River Basin.

similar to the spatial distribution of the mean annual precipitation over the period from 2000 to 2012 (Fig. 6). A clear boundary is observed in the map and is consistent with the 400-mm isohyet.

4.2. Comparison in sub-basins

We divided the entire basin into 14 sub-basins and evaluated the satellite precipitation products at both daily and monthly scales, as shown in Tables 2 and 3.

Of the near real-time datasets, 3B42RT always overestimates precipitation at the daily scale, whereas CMORPH presents a mixed pattern containing both positive and negative BIAS values that range from −19.77% to 25.74%. The gauge adjustment in 3B42V7 and CMORPH_adj significantly reduces BIAS. However, these products are not always superior over the near real-time datasets, particularly CMORPH. The ME value is the largest in sub-basin 14 for all the datasets. We suspect that this phenomenon may be caused by the low density of the gauge network in this region given that the network cannot provide sufficient benchmark data. As per a comparison of the unadjusted datasets, CMORPH exhibits a strong correlation with gauge observations; this correlation is close to the results obtained with 3B42V7 and CMORPH_adj.

As with the daily analysis, 3B42RT overestimates monthly rainfall; nevertheless, the results agree with the rain gauge observations. In most sub-basins, the values of CC (ranging from 0.64 to 0.92) are greater than those of CMORPH (ranging from 0.69 to 0.92). When the monthly rain gauge

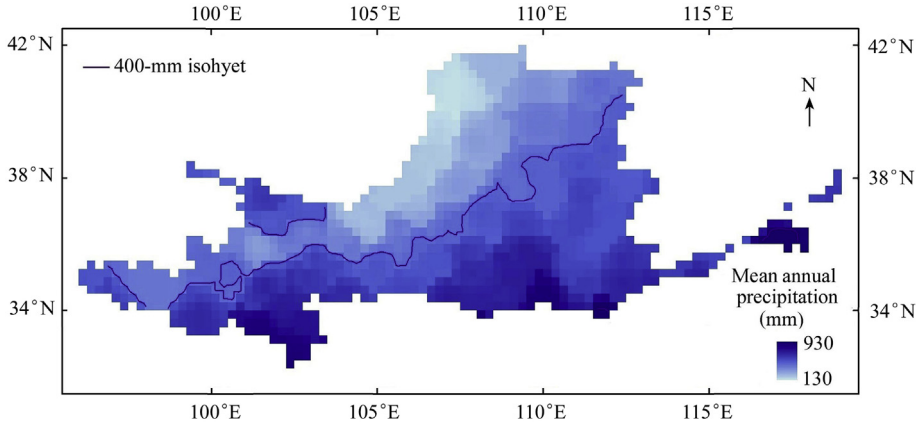

Fig. 6. Spatial distribution of mean annual precipitation based on rain gauge observations from 2000 to 2012.

observation is adjusted, the monthly 3B42V7 precipitation data fit the gauge observations fully at a monthly scale; this outcome is considerably superior to that of the daily analysis. 3B42V7 generates ideal CC values of over 0.93 in all cases; in addition, CMORPH_adj (whose CC value ranges from 0.83 to 0.97) shows more agreement with the gauge observations than CMORPH due to the gauge data adjustment. Overall, 3B42V7 is statistically similar to monthly gauge observations.

4.3. Comparison over basin

We also compared the basin-scale rainfall interpolated by gauges against the rainfall estimated based on satellites, as shown in Table 4. The scatterplots of daily and monthly satellite products versus the benchmark rainfall for the entire basin are depicted in Figs. 7 and 8, respectively. The statistics generated with the basin-averaged data are superior to the results obtained from the grid-based comparison.

Table 2
Statistical summary of four satellite precipitation estimates in sub-basins at daily scale.

Sub-basin	TMPA 3B42RT				CMORPH			
	BIAS (%)	ME (mm)	RMSE (mm)	CC	BIAS (%)	ME (mm)	RMSE (mm)	CC
1	34.75	0.75	3.46	0.35	1.65	0.02	2.00	0.51
2	34.30	0.60	3.63	0.30	5.04	0.06	2.52	0.34
3	31.12	0.29	2.30	0.37	18.61	0.15	1.85	0.42
4	12.84	0.19	4.55	0.31	−10.50	−0.12	3.74	0.32
5	26.64	0.41	4.52	0.36	−19.77	−0.19	3.44	0.38
6	20.24	0.37	4.12	0.50	−15.08	−0.19	3.58	0.51
7	27.16	0.50	3.72	0.53	−7.71	−0.10	3.16	0.54
8	21.93	0.42	3.93	0.54	−6.23	−0.09	3.42	0.55
9	17.72	0.15	2.95	0.36	18.44	0.16	2.66	0.38
10	23.89	0.38	3.80	0.47	2.73	0.03	3.44	0.48
11	31.37	0.49	3.68	0.44	4.40	0.05	3.18	0.45
12	28.81	0.51	4.04	0.48	4.71	0.06	3.54	0.50
13	29.60	0.64	4.74	0.49	3.50	0.05	3.98	0.51
14	38.80	0.86	5.78	0.42	25.74	0.47	5.05	0.42
Sub-basin	TMPA 3B42V7				CMORPH_adj			
	BIAS (%)	ME (mm)	RMSE (mm)	CC	BIAS (%)	ME (mm)	RMSE (mm)	CC
1	11.96	0.17	2.39	0.52	17.18	0.27	2.15	0.55
2	10.76	0.14	2.60	0.43	12.95	0.17	2.64	0.38
3	8.53	0.06	1.81	0.51	13.71	0.10	1.92	0.46
4	3.48	0.05	3.99	0.40	4.93	0.07	4.16	0.33
5	10.16	0.13	3.45	0.53	1.89	0.02	3.69	0.42
6	9.51	0.15	3.55	0.60	8.84	0.14	3.87	0.54
7	12.45	0.19	3.08	0.64	12.09	0.19	3.41	0.57
8	6.85	0.11	3.34	0.63	11.70	0.20	3.67	0.57
9	2.40	0.02	2.53	0.47	21.68	0.19	2.84	0.42
10	10.12	0.14	3.37	0.55	7.47	0.10	3.52	0.50
11	11.95	0.15	3.09	0.52	4.91	0.06	3.15	0.47
12	11.61	0.17	3.44	0.56	5.07	0.07	3.56	0.52
13	16.01	0.29	3.94	0.59	13.12	0.23	4.11	0.53
14	31.42	0.63	4.94	0.51	34.19	0.71	5.13	0.46

Table 3
Statistical summary of four satellite precipitation estimates in sub-basins at monthly scale.

Sub-basin	TMPA 3B42RT				CMORPH			
	BIAS (%)	ME (mm)	RMSE (mm)	CC	BIAS (%)	ME (mm)	RMSE (mm)	CC
1	34.75	25.17	70.33	0.89	1.65	0.65	19.32	0.86
2	34.30	18.22	32.42	0.86	5.04	1.85	16.03	0.87
3	31.12	8.76	16.39	0.83	18.61	4.44	13.59	0.79
4	12.84	5.83	25.22	0.81	−10.50	−3.76	22.60	0.79
5	26.64	12.54	34.60	0.64	−19.77	−5.70	25.23	0.69
6	20.24	11.25	26.31	0.85	−15.08	−5.81	25.64	0.82
7	27.16	15.35	27.96	0.85	−7.71	−2.95	22.31	0.83
8	21.93	12.91	24.06	0.90	−6.23	−2.70	19.48	0.90
9	17.72	4.59	17.13	0.80	18.44	4.82	16.64	0.78
10	23.89	11.54	21.87	0.90	2.73	1.03	18.75	0.88
11	31.37	15.03	26.20	0.90	4.40	1.51	18.15	0.89
12	28.81	15.50	25.37	0.91	4.71	1.90	18.86	0.90
13	29.60	19.39	31.92	0.90	3.50	1.67	21.69	0.89
14	38.80	26.28	45.57	0.92	25.74	14.37	31.85	0.92
Sub-basin	TMPA 3B42V7				CMORPH_adj			
	BIAS (%)	ME (mm)	RMSE (mm)	CC	BIAS (%)	ME (mm)	RMSE (mm)	CC
1	11.96	5.30	8.40	0.99	17.18	8.08	14.60	0.96
2	10.76	4.21	9.39	0.98	12.95	5.19	11.10	0.96
3	8.53	1.81	6.71	0.96	13.71	3.08	8.24	0.94
4	3.48	1.43	11.17	0.96	4.93	2.05	18.41	0.88
5	10.16	3.90	12.16	0.95	1.89	0.66	19.81	0.83
6	9.51	4.66	12.47	0.97	8.84	4.30	18.51	0.92
7	12.45	5.85	11.80	0.98	12.09	5.66	18.53	0.92
8	6.85	3.38	9.62	0.98	11.70	6.09	15.77	0.95
9	2.40	0.52	9.14	0.93	21.68	5.90	13.57	0.90
10	10.12	4.14	9.65	0.98	7.47	2.97	13.60	0.94
11	11.95	4.46	8.91	0.99	4.91	1.70	10.51	0.96
12	11.61	5.03	9.59	0.99	5.07	2.04	10.64	0.97
13	16.01	8.79	14.31	0.99	13.12	6.96	16.49	0.95
14	31.42	18.99	31.19	0.98	34.19	21.54	32.65	0.95

Table 4
Statistical summary of basin-averaged comparison of four satellite precipitation estimates over Yellow River Basin at daily and monthly scales.

Satellite precipitation product	Statistical index at daily scale							Statistical index at monthly scale			
	BIAS (%)	ME (mm)	RMSE (mm)	CC	POD	FAR	CSI	BIAS (%)	ME (mm)	RMSE (mm)	CC
TMPA 3B42RT	31.93	0.55	2.11	0.60	0.84	0.42	0.52	31.93	16.75	22.59	0.93
CMORPH	0.39	0.00	1.57	0.67	0.75	0.30	0.57	0.39	0.14	12.07	0.93
TMPA 3B42V7	7.83	0.10	1.54	0.72	0.79	0.30	0.59	7.83	3.03	5.41	0.99
CMORPH_adj	9.50	0.12	1.59	0.69	0.80	0.30	0.59	9.50	3.75	6.90	0.99

Nonetheless, the daily BIAS and ME values of the 3B42RT remain the highest among the four products, whereas those of CMORPH are the lowest. As per an analysis of the indices, 3B42V7 performs better than the others and is highly consistent with rain gauge observations (Table 4 and Fig. 7). The capability of the four products to detect rainfall events improved based on the grid-based comparison. Furthermore, the monthly estimates made by these products are highly consistent with the benchmark (Fig. 8), especially that made by 3B42V7.

We divided the daily precipitation (P) into five categories: $0 < P \leq 1$ mm, $1 < P \leq 5$ mm, $5 < P \leq 10$ mm, $10 < P \leq 20$ mm, and $P > 20$ mm. Table 5 presents the precipitation occurrence frequencies of the rain gauge observations; and 3B42RT, CMORPH, 3B42V7, and CMORPH_adj. The results show that all the CMORPH, 3B42V7, and CMORPH_adj data show much more agreement with the observations regarding precipitation occurrence frequency in different categories than 3B42RT data. However, CMORPH and CMORPH_adj underestimated the values in the high precipitation intensity (PI) range ($P > 10$ mm). By contrast, 3B42RT underestimated the minimum PI range (less than 1 mm) and overestimated the high PI range (from 1 to 20 mm). Thus, 3B42RT has the poorest performance in the Yellow River Basin among the products. According to Table 6, we can see that the precipitation contribution of the TMPA data fit better than the CMORPH data.

Fig. 9 shows the monthly precipitation time series derived from 2000 to 2012. 3B42RT significantly overestimated precipitation during the period from June to September.

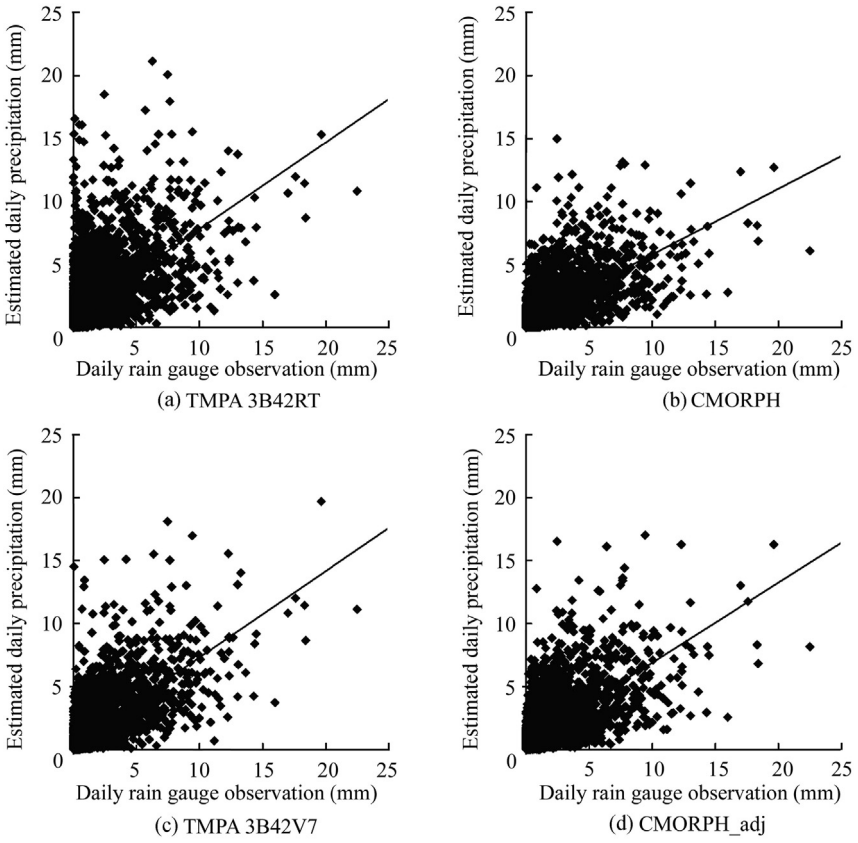

Fig. 7. Scatterplots for comparison of average daily precipitation over basin.

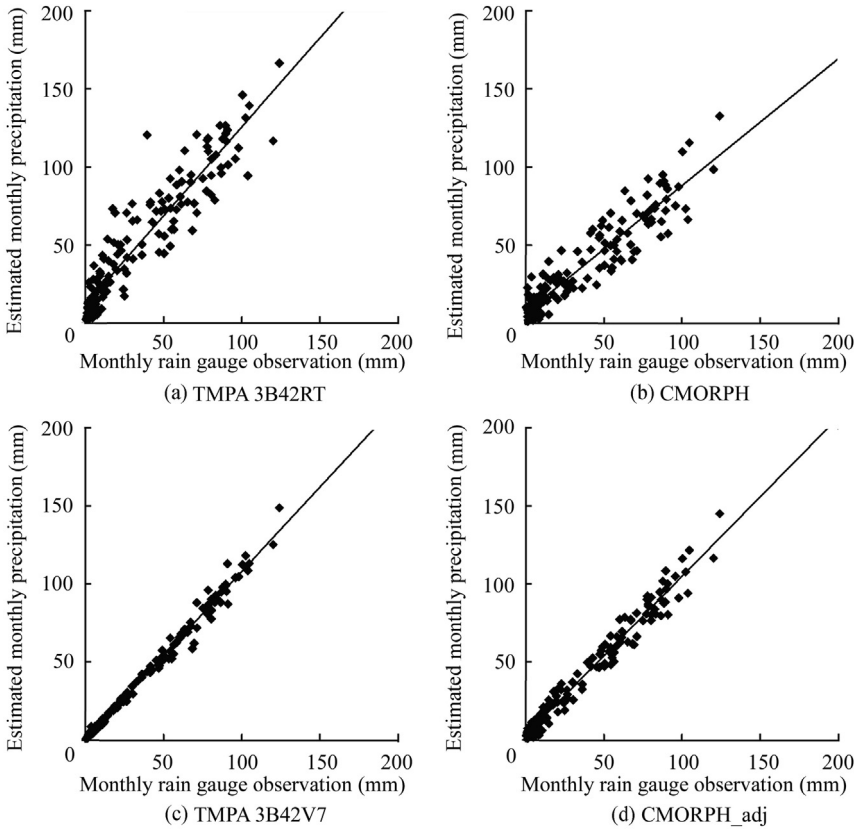

Fig. 8. Scatterplots for comparison of average monthly precipitation over basin.

Table 5
Precipitation occurrence frequencies of rain gauge observations, and 3B42RT, CMORPH, 3B42V7, and CMORPH_adj in terms of basin average within Yellow River Basin.

Daily precipitation category (mm)	Precipitation occurrence frequency (%)				
	Rain gauge observation	TMPA 3B42RT	CMORPH	TMPA 3B42V7	CMORPH_adj
$0 < P \leq 1$	69.80	56.15	67.50	65.96	65.64
$1 < P \leq 5$	24.16	34.66	28.34	28.24	28.64
$5 < P \leq 10$	5.16	7.51	3.80	5.01	5.18
$10 < P \leq 20$	0.85	1.64	0.36	0.77	0.53
$P > 20$	0.02	0.04	0.00	0.02	0.00

Table 6
Precipitation contributions of rain gauge observations, and 3B42RT, CMORPH, 3B42V7, and CMORPH_adj in terms of basin average within Yellow River Basin.

Daily precipitation category (mm)	Precipitation contribution (%)				
	Rain gauge observation	TMPA 3B42RT	CMORPH	TMPA 3B42V7	CMORPH_adj
$0 < P \leq 1$	12.27	10.04	20.98	13.73	16.15
$1 < P \leq 5$	47.53	48.36	54.56	52.26	51.35
$5 < P \leq 10$	30.52	29.40	20.80	26.05	27.17
$10 < P \leq 20$	9.27	11.69	3.66	7.55	5.32
$P > 20$	0.41	0.51	0.00	0.41	0.00

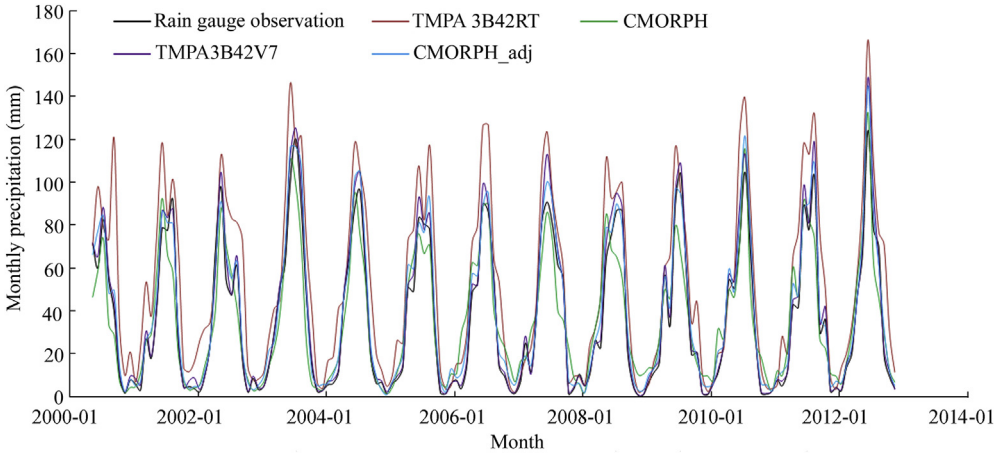

Fig. 9. Monthly time series of precipitation for rain gauge observations and satellite estimates throughout Yellow River Basin from 2000 to 2012.

CMORPH precipitation data predicted the flood season in advance, and the values generated are close to the observations. 3B42V7 fits best with the rain gauge observations in all cases. Although CMORPH_adj fits these observations better than CMORPH, the accuracy of the former is lower than that of 3B42V7. These results indicate that 3B42V7 may be the most appropriate dataset for use in hydrological research; the CMORPH_adj can be applied as well and CMORPH performs much better than 3B42RT in the Yellow River Basin.

5. Conclusions

In this study, we compared four widely used satellite precipitation products, namely, TMPA 3B42RT, CMORPH, TMPA 3B42V7, and CMORPH_adj, against rain gauge observations across the Yellow River Basin during the period from 2000 to 2012. We evaluated and compared the error characteristics of these products at different spatial and temporal scales, and the main conclusions are as follows:

(1) The validation statistics show that all the satellite precipitation products overestimated precipitation, particularly the 3B42RT. At the daily scale, the products exhibit a low correlation with ground rain gauge data, while the monthly CC values have significantly improved. Moreover, the gauge adjustment significantly reduces the BIAS in 3B42V7 and CMORPH_adj, and both research products, particularly 3B42V7, perform better than the near real-time products.

(2) According to the spatial distribution of statistical indices, these values are optimized in the southeast and decline toward the northwest, and the trend is similar to the spatial distribution of mean annual precipitation over the period from 2000 to 2012. A clear boundary is observed and it is consistent with the 400-mm isohyet.

(3) As per the categorical statistics, all four products effectively detect rainfall events, although CMORPH and CMORPH_adj underestimate the values in the high PI range (more than 10 mm). By contrast, 3B42RT underestimates the lowest PI range (less than 1 mm) and overestimates the high PI range (from 1 to 20 mm).

(4) For the four satellite precipitation products, 3B42V7 may be the most appropriate dataset that can be used in hydrological research, and the CMORPH_adj is applicable as well. Of the two near real-time datasets, CMORPH performs better than 3B42RT over the Yellow River Basin.

Overall, these results provide satellite product users with insights into the performance of these most recent satellite precipitation products for water resources applications and hydrologic monitoring in other similar regions in China. This information also facilitates the use of GPM data in the future.

References

Bartier, P.M., Keller, C.P., 1996. Multivariate interpolation to incorporate thematic surface data using inverse distance weighting (IDW). Comput. Geosci. 22(7), 795−799. http://dx.doi.org/10.1016/0098-3004(96)00021-0.

Cai, Y.C., Jin, C.J., Wang, A.Z., Guan, D.X., Wu, J.B., Yuan, F.H., Xu, L.L., Bu, C.Q., 2014. Accuracy evaluation of the TRMM satellite-based precipitation data over the mid-high latitudes. Chin. J. Appl. Ecol. 25(11), 3296−3306 (in Chinese).

Chen, F., Liu, C., 2012. Estimation of the spatial rainfall distribution using inverse distance weighting (IDW) in the middle of Taiwan. Paddy Water Environ. 10(3), 209−222. http://dx.doi.org/10.1007/s10333-012-0319-1.

Ebert, E.E., Janowiak, J.E., Kidd, C., 2007. Comparison of near-real time precipitation estimates from satellite observations and numerical models. Bull. Am. Soc. 88(1), 47−64. http://dx.doi.org/10.1175/BAMS-88-1-47.

Ferreira, V.G., Andam-Akorful, S.A., He, X.F., Xiao, R.Y., 2014. Estimating water storage changes and sink terms in Volta Basin from satellite missions. Water Sci. Eng. 7(1), 5−16. http://dx.doi.org/10.3882/j.issn.1674-2370.2014.01.002.

Hao, Z.C., Tong, K., Liu, X.L., Zhang, L.L., 2014. Capability of TMPA products to simulate streamflow in upper Yellow and Yangtze River basins on Tibetan Plateau. Water Sci. Eng. 7(3), 237−249. http://dx.doi.org/10.3882/j.issn.1674-2370.2014.03.001.

Hu, Q.F., Yang, D.W., Li, Z., Mishra, A.K., Wang, Y.T., Yang, H.B., 2014. Multi-scale evaluation of six high-resolution satellite monthly rainfall estimates over a humid region in China with dense rain gauges. Int. J. Remote Sens. 35(4), 1274−1294. http://dx.doi.org/10.1080/01431161.2013.876118.

Huffman, G.J., Adler, R.F., Bolvin, D.T., Gu, G., Nelkin, E.J., Bowman, K.P., Hong, Y., Stocker, E.F., Wolff, D.B., 2007. The TRMM multi-satellite precipitation analysis (TMPA): Quasi-global, multi-year, combined-sensor precipitation estimates at fine scales. J. Hydrometeorol. 8, 38−55. http://dx.doi.org/10.1175/JHM560.1.

Jiang, S.H., Ren, L.L., Yong, B., Yang, X.L., Shi, L., 2010. Evaluation of high-resolution satellite precipitation products with surface rain gauge observations from Laohahe Basin in northern China. Water Sci. Eng. 3(4), 405−417. http://dx.doi.org/10.3882/j.issn.1674-2370.2010.04.004.

Joyce, R.J., Janowiak, J.E., Arkin, P.A., Xie, P., 2004. CMORPH: A method that produces global precipitation estimates from passive microwave and infrared data at high spatial and temporal resolution. J. Hydrometeorol. 5, 487−503. http://dx.doi.org/10.1175/1525-7541(2004)005<0487:CAMTPG>2.0.CO;2.

Li, X.H., Zhang, Q., Shao, M., 2012. Spatio-temporal distribution of precipitation in Poyang Lake Basin based on TRMM data and precision evaluation. Prog. Geogr. 1(9), 1164−1170 (in Chinese).

Li, Z., Yang, D.W., Hong, Y., 2013. Multi-scale evaluation of high-resolution multi-sensor blended global precipitation products over the Yangtze River. J. Hydrol. 500, 157−169. http://dx.doi.org/10.1016/j.jhydrol.2013.07.023.

Li, Z., Yang, D.W., Gao, B., Jiao, Y., Hong, Y., Xu, T., 2015. Multi-scale hydrologic applications of the latest satellite precipitation products in the Yangtze River Basin using a distributed hydrologic model. J. Hydrometeorol. 26, 407−426. http://dx.doi.org/10.1175/JHM-D-14-0105.1.

Liu, Z., 2015. Comparison of precipitation estimates between Version 7 3-hourly TRMM multi-satellite precipitation analysis (TMPA) near-real-time and research products. Atmos. Res. 153, 119−133. http://dx.doi.org/10.1016/j.atmosres.2014.07.032.

Lo Conti, F., Hsu, K.L., Noto, L.V., Sorooshian, S., 2014. Evaluation and comparison of satellite precipitation estimates with reference to a local area in the Mediterranean Sea. Atmos. Res. 138, 189−204. http://dx.doi.org/10.1016/j.atmosres.2013.11.011.

Meng, J., Li, L., Hao, Z.C., Wang, J.H., Shao, Q.X., 2014. Suitability of TRMM satellite rainfall in driving a distributed hydrological model in the source region of Yellow River. J. Hydrol. 509, 320−332. http://dx.doi.org/10.1016/j.jhydrol.2013.11.049.

Nastos, P.T., Kapsomenakis, J., Douvis, K.C., 2013. Analysis of precipitation extremes based on satellite and high-resolution gridded data set over Mediterranean Basin. Atmos. Res. 131, 46−59. http://dx.doi.org/10.1016/j.atmosres.2013.04.009.

Petersen, W.A., Rutledge, S.A., 2001. Regional variability in tropical convection: Observations from TRMM. J. Clim. 14(17), 3566−3586. http://dx.doi.org/10.1175/1520-0442(2001)014<3566:RVITCO>2.0.CO;2.

Sadiq, I.K., Hong, Y., Gourley, J.J., Muhammad, U.K.K., Yong, B., Humberto, J.V., 2014. Evaluation of three high-resolution satellite precipitation estimates: Potential for monsoon monitoring over Pakistan. Adv. Space Res. 54(4), 670−684. http://dx.doi.org/10.1016/j.asr.2014.04.017.

Shen, Y., Xiong, A.Y., Wang, Y., Xie, P.P., 2010. Performance of high-resolution satellite precipitation products over China. J. Geophys. Res. 115(D2), D02114. http://dx.doi.org/10.1029/2009JD012097.

Shen, Y., Zhao, P., Pan, Y., Yu, J.J., 2014. A high spatiotemporal gauge-satellite merged precipitation analysis over China. J. Geophys. Res. Atmos. 119(6), 3063−3075. http://dx.doi.org/10.1002/2013JD020686.

Tong, K., Su, F.G., Yang, D.Q., Hao, Z.C., 2014. Evaluation of satellite precipitation retrievals and their potential utilities in hydrologic modeling over the Tibetan Plateau. J. Hydrol. 519, 423−437. http://dx.doi.org/10.1016/j.jhydrol.2014.07.044.

Xue, X.W., Hong, Y., Limaye, A.S., Gourley, J.J., Huffmane, G.J., Sadiq, I.K., Chhimi, D., Chen, S., 2013. Statistical and hydrological evaluation of TRMM-based multi-satellite precipitation analysis over the Wangchu Basin of Bhutan: Are the latest satellite precipitation products 3B42V7 ready for use in ungauged basins? J. Hydrol. 499, 91−99. http://dx.doi.org/10.1016/j.jhydrol.2013.06.042.

Yong, B., Ren, L.L., Hong, Y., Wang, J.H., Gourley, J.J., Jiang, S.H., Chen, X., Wang, W., 2010. Hydrologic evaluation of multisatellite precipitation analysis standard precipitation products in basins beyond its inclined latitude band: A case study in Laohahe Basin, China. Water Resour. Res. 46(7), W07542. http://dx.doi.org/10.1029/2009WR008965.

Yong, B., Chen, B., Gourley, J.J., Ren, L.L., Hong, Y., Chen, X., Wang, W.G., Chen, S., Gong, L.Y., 2014. Intercomparison of the Version-6 and Version-7 TMPA precipitation products over high and low latitudes basins with independent gauge networks: Is the newer version better in both real-time and post-real-time analysis for water resources and hydrologic extremes? J. Hydrol. 508, 77−87. http://dx.doi.org/10.1016/j.jhydrol.2013.10.050.

Yong, B., Liu, D., Gourley, J.J., Tian, Y., Huffman, G.J., Ren, L.L., Hong, Y., 2015. Global view of real-time TRMM multi satellite precipitation analysis: Implications for its successor global precipitation measurement mission. Bull. Am. Meteorol. Soc. 96(2), 283−296. http://dx.doi.org/10.1175/BAMS-D-14-00017.1.

Zhuang, L.W., Wang, S.L., 2003. Spatial interpolation methods of daily weather data in Northeast China. J. Appl. Meteorol. Sci. 14(5), 605−615 (in Chinese).